Figure legends

Fig. 1.

A hepatocellular carcinoma that exhibited a marked response to sorafenib treatment harbors *FGF3*/*FGF4* gene amplification. (A) Abdominal CT images obtained upon pre-treatment (left panel) and two months after treatment (right panel). (B) Comparative genomic hybridization analysis of the HCC tumor. Paired background liver tissue was used as a reference sample. A gain of genomic copy number (> 4 copies, red) and a loss (< 0.5 copies, blue) were shown by the indicated colors. (C) Whole copy numbers of chromosome 11 are shown. A highly amplified region is described in the lower panel. (D) Western blot analysis of FGF3 (Arrow) in HCC and paired background liver samples. IB, immunoblotting. Liver, paired background liver.

Fig. 2.

FGF3/*FGF4* gene amplification is frequently observed in responders to sorafenib in HCC. (A) *FGF3*/*FGF4* gene amplification was determined using the TaqMan copy number assay in DNA samples obtained from 48 HCC samples that had been treated with sorafenib. *FGF3* amplification of over 5 copies was observed in

3 of the responders to sorafenib. *, CR+PR *vs.* SD+PD. (B) *FGF3*/*FGF4* gene amplification mediates the overexpression of *FGF3*/*FGF4* mRNA. The mRNA expression levels of *FGF3* and *FGF4* were examined in nine HCC samples that were available as frozen samples among forty eight HCC samples that were treated with sorafenib. Rel. mRNA, *target gene*/*GAPD* x10^6.

Fig. 3.

Fluorescence *in situ* hybridization analysis of *FGF3*-amplified HCC. Green, *CEN11P* locus; Red, *FGF3* locus; No., sample numbers; Amp, gene amplification. High-power images are presented for a single cancer cell.

Fig. 4.

FGF3/*FGF4* gene amplification in a series of HCC samples without sorafenib treatment. (A) A TaqMan copy number assay for *FGF3* and *FGF4* was used to examine DNA samples obtained from 82 surgical specimens. Human normal genomic DNA was used as a normal control. Well, well-differentiated HCC; Mod, moderately differentiated HCC; Poor, poorly differentiated HCC.

Fig. 5.

FGF3 and FGF4 overexpression and drug sensitivity to sorafenib *in vitro* and *in vivo*. (A) Growth inhibitory assay examining sorafenib in various cancer cell lines *in vitro*. The growth inhibitory effect of sorafenib was examined using an MTT assay. The IC_{50} values of each cell line are shown in the graph. The black bars show that the IC_{50} values were below 1 μM. Amp, gene amplification. (B) Cancer cell lines stably overexpressing *EGFP*, *FGF3* or *FGF4* were established and designated as A549/EGFP, A549/FGF3 and A549/FGF4. Western blotting confirmed that exogenously expressed FGF3 and FGF4 were secreted into the culture medium. IB, Immunoblotting; Sup., supernatant. (C) The 3T3 cells were exposed to indicated concentrations of sorafenib for 2 hours and were then stimulated with FGF4 conditioned medium for 20 minutes. (D) Mice inoculated with A549/EGFP, A549/FGF3 or A549/FGF4 (n=20 each) were treated with a low dose of sorafenib (n=10, 15 mg/kg/day, p.o.) or without (n=10, vehicle control, p.o.). *p<0.05.

Fig. 1.

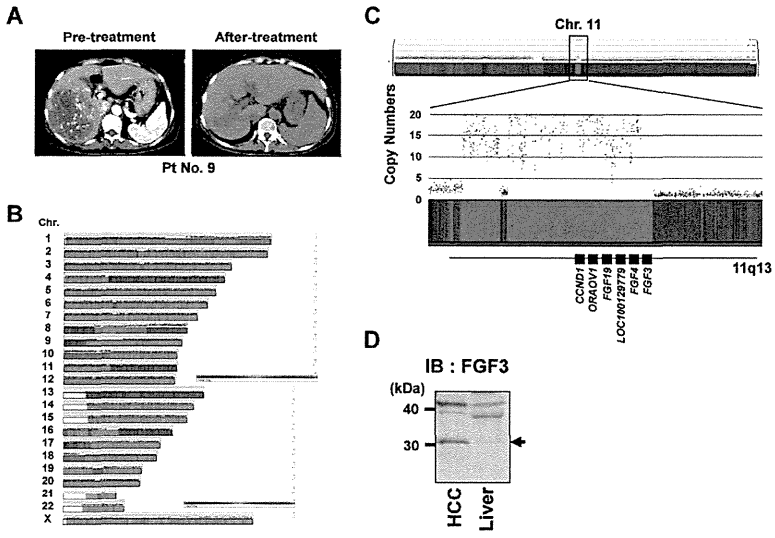

99x75mm (300 x 300 DPI)

Fig. 2.

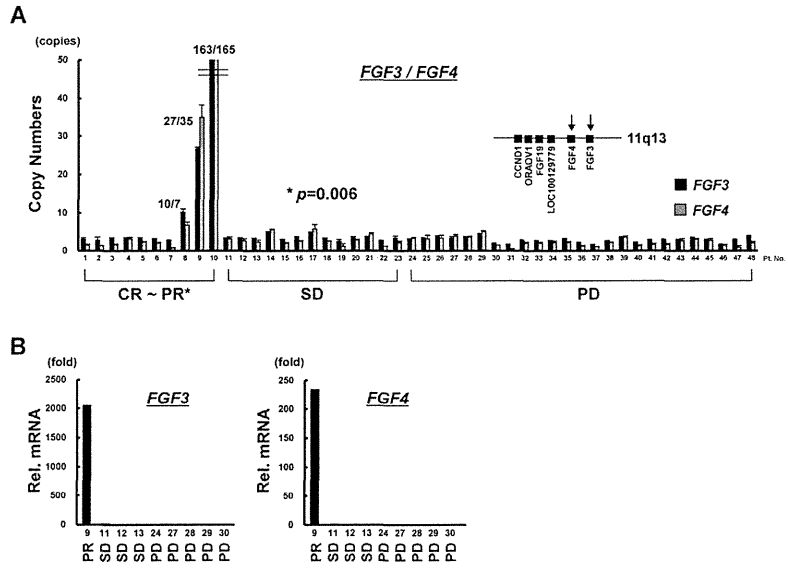

99x75mm (300 x 300 DPI)

Fig. 3.

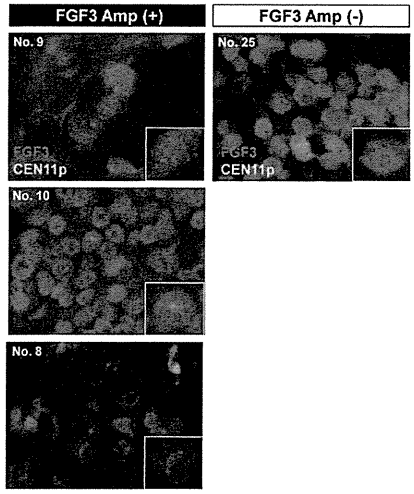

99x75mm (300 x 300 DPI)

Fig. 4.

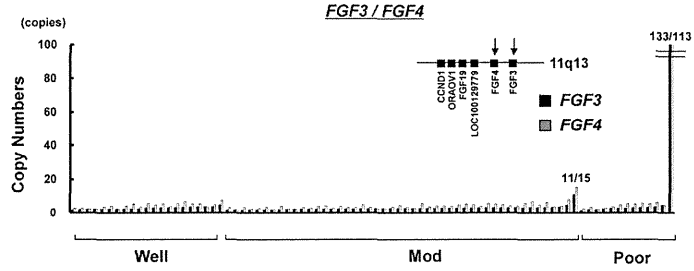

99x75mm (300 x 300 DPI)

Fig. 5.

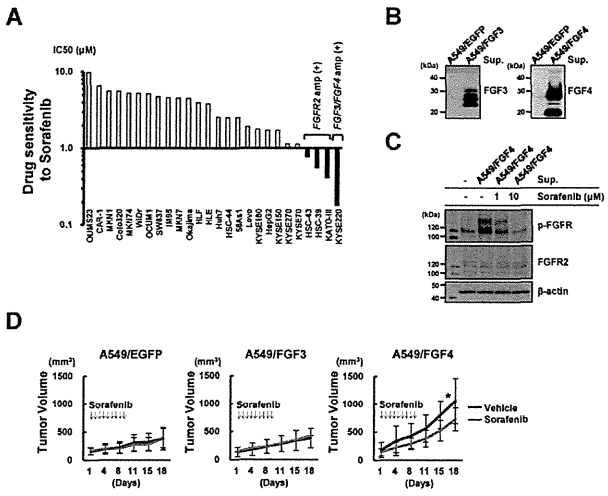

99x75mm (300 x 300 DPI)

Original Paper

Intraepithelial Ductal Spread in Colorectal Carcinoma Liver Metastasis

Toshifumi Wakai[1], Pavel V Korita[2], Yoichi Ajioka[2], Makoto Inoue[1], Masaaki Takamura[3], Kohei Akazawa[4], Yoshio Shirai[1] and Katsuyoshi Hatakeyama[1]

[1]Division of Digestive and General Surgery, [2]Division of Molecular and Diagnostic Pathology, [3]Division of Gastroenterology and Hepatology and [4]Department of Medical Informatics, Niigata University Graduate School of Medical and Dental Sciences, Chuo-ku, Niigata, Japan

Corresponding Author: Yoichi Ajioka, MD, PhD, Division of Molecular and Diagnostic Pathology, Niigata University Graduate School of Medical and Dental Sciences, 1-757 Asahimachi-dori, Chuo-ku, Niigata, 951-8510, Japan

Tel: +81252272093, Fax: +81252270760, E-mail: ajioka@med.niigata-u.ac.jp

ABSTRACT

Background/Aims: This study aimed to evaluate the usefulness of immunohistochemical combinations for discrimination between intraepithelial ductal spread of colorectal carcinoma liver metastasis (CRLM) and that of intrahepatic cholangiocarcinoma (ICC).

Methodology: A retrospective analysis of resected specimens from 151 patients with CRLM and 28 patients with ICC was conducted. Intraepithelial ductal spread along the bile ducts was judged positive when tumor cells spreading along the intact basement membranes of intrahepatic bile ducts. We evaluated immunoreactivity of cytokeratin (CK) 7, CK20, CDX2, MUC2, MUC5AC and human gastric mucin (HGM).

Results: Of the 151 patients with CRLM, 21 had intrahepatic bile duct involvement verified histologically. Intraepithelial ductal spread was detected in 17 of 21 (81%) patients with CRLM with bile duct involvement, whereas it was detected in 22 of 28 (79%) patients with ICC. CK20-positive/CK7-negative immunophenotype demonstrated a high accuracy of 95% for evaluation of intraepithelial ductal spread from CRLM. CK7-positive/CK20-negative immunophenotype demonstrated the highest accuracy of 85% for evaluation of intraepithelial ductal spread from ICC.

Conclusion: Intraepithelial ductal spread is a common feature of CRLM with bile duct involvement. Immunohistochemical combination of CK7 and CK20 is useful for discrimination between intraepithelial ductal spread of CRLM and that of ICC.

KEY WORDS: Liver neoplasms; Colorectal carcinoma liver metastasis; Intrahepatic cholangiocarcinoma; Intraepithelial spread; Immunohistochemistry

ABBREVIATIONS: Colorectal Carcinoma Liver Metastasis (CRLM); Intrahepatic Cholangiocarcinoma (ICC); Cytokeratin (CK); Human Gastric Mucin (HGM); Computed Tomography (CT); CT Arterial Portography (CTAP); Endoscopic Retrograde Cholangiopancreatography (ERCP); Percutaneous Transhepatic Cholangiography (PTC)

INTRODUCTION

Since Riopel *et al.* (1) reported eight cases of colonic adenocarcinoma metastatic to the liver that demonstrated prominent spread throughout the biliary tree along intact basement membranes, intraepithelial ductal spread along the bile ducts is recognized behavior of colorectal carcinoma liver metastasis (CRLM), mimicking primary intrahepatic cholangiocarcinoma (ICC). As intraepithelial ductal spread from CRLM closely resembles high-grade dysplasia (*i.e.* carcinoma *in situ*) of the extrahepatic and intrahepatic bile ducts, Riopel *et al.* (1) emphasized that this pattern of intraepithelial ductal spread may make it difficult to discriminate CRLM from primary biliary neoplasms. Although several authors demonstrated that cytokeratin (CK) 7 (specific for biliary epithelium) and CK20 (specific for intestinal epithelium) immunophenotypes are useful for discrimination between CRLM and primary ICC (2-8), a few previous reports which focused on immunohistochemical discrimination of intraepithelial ductal spread from CRLM were case reports (9-12). Therefore, little is known regarding this pattern of intraepithelial ductal spread from CRLM.

CDX2 and MUC2 immunophenotypes are specific markers for intestinal epithelium and adenocarcinoma of the intestinal origin, whereas gastric mucin MUC5AC and human gastric mucin (HGM) immunophenotypes have been proposed as potential markers for ICC (13-16). We evaluated immunoreactivity of CK profile (CK 7 and CK20) and mucin profile (CDX2, MUC2, MUC5AC and HGM) focused on intraepithelial ductal spread of CRLM and that of ICC. This study aimed to evaluate the usefulness of immunohistochemical combinations for discrimination between intraepithelial ductal spread of CRLM and that of ICC.

METHODOLOGY

We examined a total of 179 liver tumors consisting of 151 CRLM and 28 ICC. These tumors came from consecutive Japanese patients who underwent surgical resection as an initial treatment at the Niigata University Medical and Dental Hospital, Niigata, Japan, from January 1990 through December 2009. The patients included 123 men and 56 women with a median age of 66 years (range, 32-82 years). Of 28 patients with ICC, 2 patients had a history of colonic adenocarcinoma. The final

Hepato-Gastroenterology 2011; 58:583-588

diagnosis of CRLM and ICC was based on clinical (medical history, follow-up) and radiological data, with consistent histology. The study protocol and the use of human samples were approved by the Institutional Review Board of Niigata University Medical and Dental Hospital, and written informed consent was obtained from all patients involved in the current study.

Radiographical data were available for all patients. These studies included liver ultrasonography, abdominal computed tomography (CT), CT arterial portography (CTAP), endoscopic retrograde cholangiopancreatography (ERCP) and/or percutaneous transhepatic cholangiography (PTC). When bile duct dilatation and/or intrabiliary filling defects were detected on CT images (**Figure 1A**), ERCP was performed for these conditions to investigate the involvement of biliary tree (**Figure 1B**).

Resected specimens were submitted to the Department of Surgical Pathology in our hospital for histological evaluation. In each resected specimen, all available sections (median, 7 sections; range, 2-19 sections) were examined to evaluate intraepithelial ductal spread along the bile ducts histologically. In patients with CRLM, the original tissue sections of primary colorectal carcinoma were available for review. Intraepithelial ductal spread from CRLM was judged positive when tumor cells spreading along the intact basement membranes of intrahepatic bile ducts replaced non-neoplastic biliary epithelium (**Figure 2E**). In the current series, high-grade dysplasia and carcinoma *in situ* were treated as intraepithelial ductal spread of ICC (**Figure 3E**).

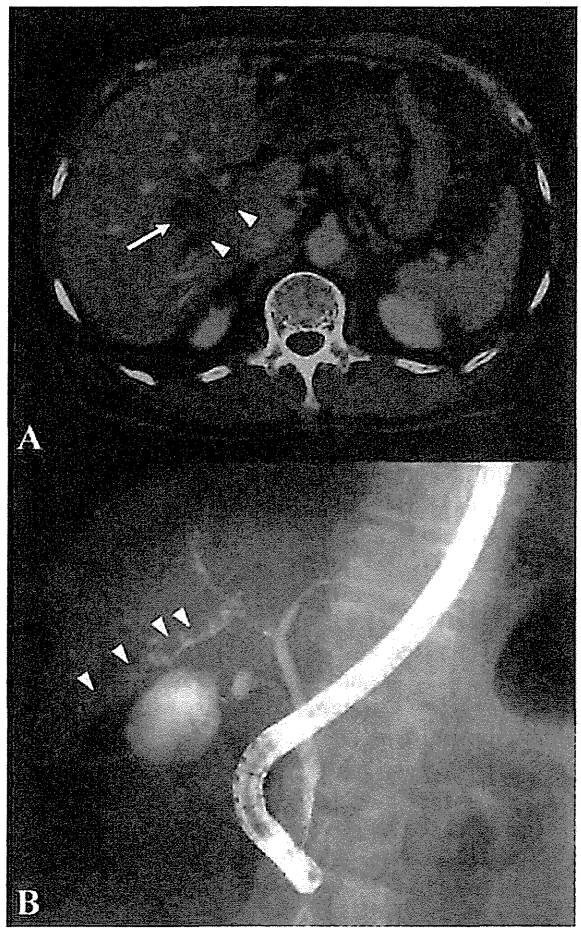

FIGURE 1
Radiological images of patient with colorectal carcinoma liver metastasis (CRLM). (**A**) Abdominal computed tomography (CT) depicts a low density mass (arrow) and dilatation of the posterior intrahepatic bile ducts (arrowheads). (**B**) Endoscopic retrograde cholangiography (ERC) demonstrates intrabiliary filling defects (arrows) within the posterior intrahepatic bile ducts.

One or two representative paraffin-embedded block(s) with the presence of intraepithelial ductal spread along the bile ducts was selected for immunohistochemistry. Nine serial 3-μm sections were re-cut and prepared from each block: one for hematoxylin-eosin staining, one for double staining with hematoxylin-eosin and Victoria blue, six for immunohistochemical staining and one as a negative control. One surgical pathologist (Y.A.) blinded to the clinical details assessed each section.

Paraffin sections were deparaffinized and rehydrated and then microwaved at 500W for 21min or autoclaved at 121°C for 20min in 10mmol/L sodium citrate buffer (pH 6.0) to retrieve antigenic activity. Endogenous peroxidase activity was inhibited by incubation with 0.3% hydrogen peroxide in methanol for 20min. After blocking any non-specific reactions with 10% normal goat serum, sections were incubated overnight at 4°C with the following antibodies: mouse monoclonal antibody against CK7 (Dako, Glostrup, Denmark; dilution at 1:100), mouse monoclonal antibody against CK20 (Dako, Glostrup, Denmark; dilution at 1:100), mouse monoclonal antibody against CDX2 protein (BioGenex Laboratories Inc., San Ramon, CA, USA; dilution at 1:200), mouse monoclonal antibody against Human Muc-2 glycoprotein (Novocastra Laboratories Ltd., Newcastle upon Tyne, UK; dilution at 1:300), mouse monoclonal antibody against Human Muc-5AC glycoprotein (Novocastra Laboratories Ltd., Newcastle upon Tyne, UK; dilution at 1:100) and mouse monoclonal antibody against HGM (Novocastra Laboratories Ltd., Newcastle upon Tyne, UK; dilution at 1:50). The sections were then incubated at room temperature for 30min with goat anti-mouse immunoglobulin conjugated to a peroxidase-labeled amino acid polymer (Simple Stain MAX-PO, MULTI; Nichirei Biosciences, Tokyo, Japan). Diaminobenzidine was used as the chromogen, and the sections were counterstained with hematoxylin. Non-neoplastic epithelium of the intrahepatic bile ducts was used as internal positive control for CK7. Intestinal epithelium was used as the positive control for CK20, MUC2 and CDX2, whereas gastric epithelium was used as the positive control for MUC5AC and HGM. For the negative control, normal mouse immunoglobulin was substituted for each primary antibody.

Immunoreactivity for each antibody was evaluated focused on intraepithelial ductal spread along the bile ducts. CK7, CK20, MUC2 or MUC5AC expression was defined as the presence of cytoplasmic immunoreactivity in the tumor cells, whereas CDX2 expression was defined as the presence of nuclear immunoreactivity according to the criteria of Nagata *et al.* (17). HGM expression was defined as the presence of cytoplasmic and/or apical membranous

immunoreactivity in the tumor cells according to the criteria of Shiroshita *et al.* (18). The expression of CK7, CK20, CDX2, MUC2, MUC5AC or HGM was judged positive when either single tumor cells or cell clusters showed immunoreactivity for each antibody, whereas it was judged negative when no immunoreactivity for each antibody was observed throughout the examined areas of intraepithelial ductal spread.

Medical records were obtained for all 179 patients (151 patients with CRLM and 28 patients with ICC). Categorical variables were compared by the Fisher exact test. The sensitivity, specificity and accuracy of immunophenotypes were calculated for the discrimination between intraepithelial ductal spread from CRLM and that from ICC. All statistical evaluations were performed using the PASW Statistics 17 software package (SPSS Japan, Tokyo, Japan). All tests were 2-tailed and a p value <0.05 was considered statistically significant.

RESULTS

Of the 151 patients with CRLM, 21 had intrahepatic bile duct involvement verified histologically. Intraepithelial ductal spread, characterized by tumor cells spreading along the intact basement membranes of intrahepatic bile ducts replacing non-neoplastic biliary epithelium (**Figure 2E**), was detected in 17 of 21 (81%) patients with CRLM with intrahepatic bile duct involvement. Of the 28 patients with ICC, intraepithelial ductal spread, characterized by high-grade dysplasia or carcinoma *in situ* (**Figure 3E**), was detected in 22 patients with ICC.

Immunophenotypes in the examined areas of intraepithelial ductal spread were comparable with immunophenotypes in main hepatic tumors of CRLM (**Figure 2**) and ICC (**Figure 3**). Immunohistochemical analyses of each monoclonal antibody focused on intraepithelial ductal spread from CRLM (n=17) and ICC (n=22) were summarized in **Table 1**. Positive expression of CK20 (p<0.001) and CDX2 (p<0.001) was significantly associated with intraepithelial ductal spread from CRLM, whereas positive expression of CK7 (p<0.001), MUC5AC (p<0.001) and HGM (p<0.001) was significantly associated with intraepithelial ductal spread from ICC. Among 22 patients with ICC with intraepithelial ductal spread along the bile ducts, 6 (27%), 9 (41%) and 8 (36%) had positive expression of CK20, CDX2 and MUC2, respectively (**Table 1**). Thus, intestinal phenotype, characterized by expression of CK20, CDX2 (**Figure 3H**) and MUC2 was occasionally observed in the areas of intraepithelial ductal spread of ICC.

Immunohistochemical combinations were assessed in the areas of intraepithelial ductal spread from CRLM. The sensitivity, specificity and accuracy of CDX2-positive/CK7-negative immunophenotype were 100%, 95% and 97%, respectively. The sensitivity, specificity and accuracy of CK20-positive/CK7-negative immunophenotype were 94%, 95% and 95%, respectively. CDX2-positive/CK7-negative immunophenotype demonstrated the highest accuracy for evaluation of intraepithelial ductal spread from CRLM.

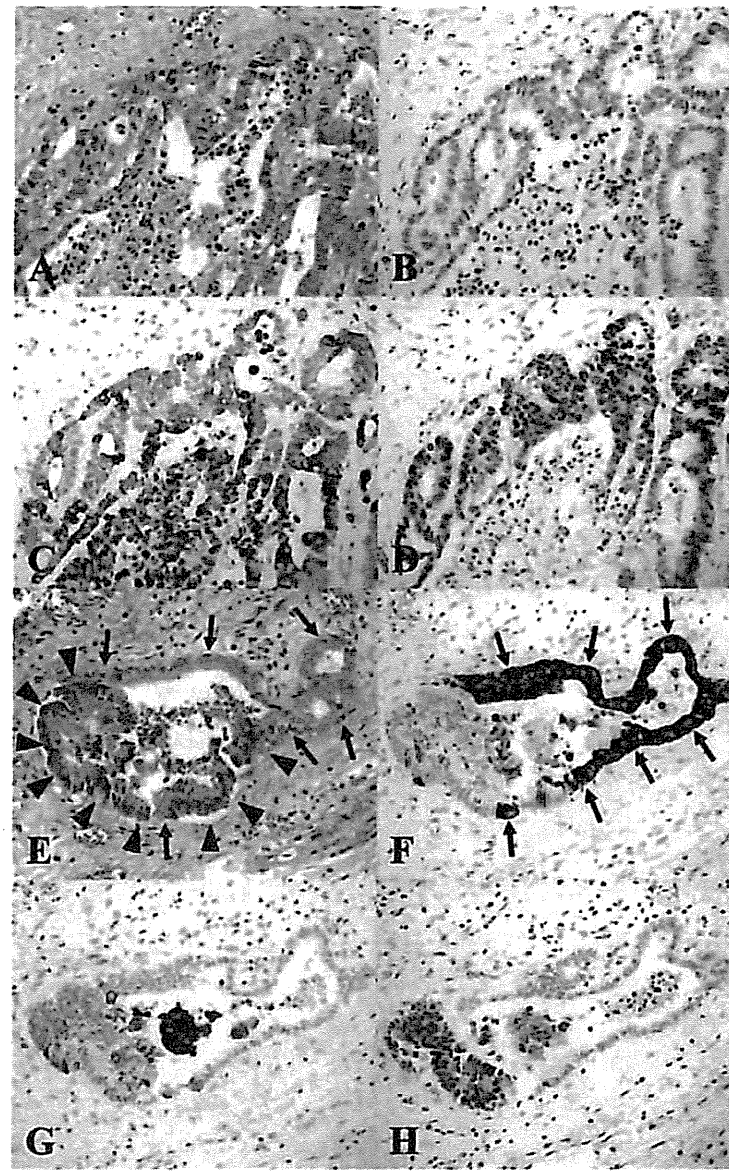

FIGURE 2 Immunophenotypes in colorectal carcinoma liver metastasis (CRLM) with intraepithelial ductal spread along the bile ducts. Tumor cells of main tumor of CRLM (**A–D**) and intraepithelial ductal spread of CRLM (**E–H**) demonstrate positive immunoreactivity for CK20 and CDX2, but negative immunoreactivity for CK7. Intraepithelial ductal spread from CRLM (arrowheads) shows replacement of non–neoplastic biliary epithelium along intact basement membranes (**E**). The remnant non–neoplastic biliary epithelium (arrows) demonstrates positive immunoreactivity for CK7 (**E** and **F**). Double staining with hematoxylin–eosin and Victoria Blue (**A** and **B**). CK7–immunohistochemical staining (**C** and **G**). CK20–immunohistochemical staining (**B** and **F**). CDX2–immunohistochemical staining (**D** and **H**).

Immunohistochemical combinations were assessed in the areas of intraepithelial ductal spread from ICC. The sensitivity, specificity and accuracy of CK7-positive/CK20-negative immunophenotype was 73%, 100% and 85%, respectively. The sensitivity, specificity and accuracy of CK7-positive/CDX2-negative immunophenotype was 59%, 100% and 77%, respectively. CK7-positive/CK20-negative immunophenotype demonstrated the highest accuracy for evaluation of intraepithelial ductal spread from ICC.

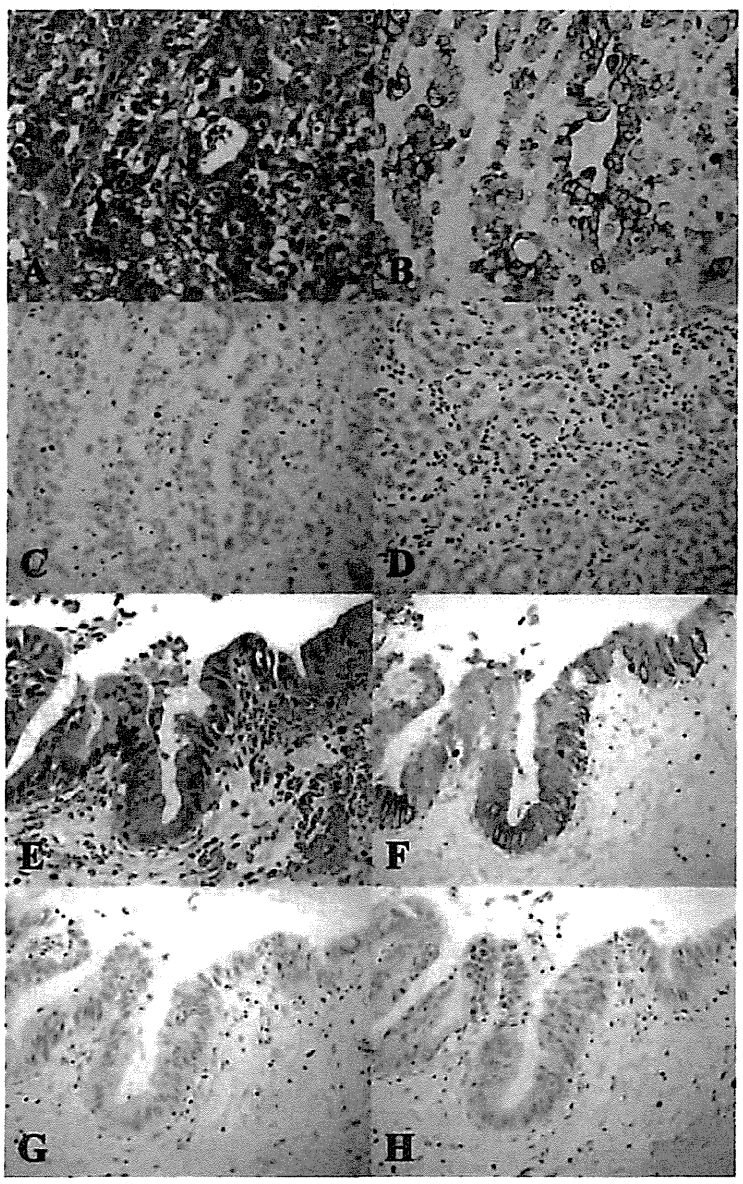

FIGURE 3 Immunophenotypes in primary intrahepatic cholangiocarcinoma (ICC) with intraepithelial ductal spread. Tumor cells of primary ICC (**A–D**) demonstrate positive immunoreactivity for CK7, but negative immunoreactivity for CK20 and CDX2. Intraepithelial ductal spread of ICC (**E–H**) demonstrates positive immunoreactivity for CK7 and CDX2, but negative immunoreactivity for CK20. Double staining with hematoxylin–eosin and Victoria Blue (**A** and **E**). CK7–immunohistochemical staining (**B** and **F**). CK20–immunohistochemical staining (**C** and **G**). CDX2–immunohistochemical staining (**D** and **H**).

In the current series, 2 patients with ICC had a past history of surgical resection for colorectal adenocarcinoma. One patient had intraepithelial ductal spread along the bile ducts (**Figure 3E-H**). Tumor cells of primary ICC (**Figure 3A**) showed positive expression of CK7 (**Figure 3B**), whereas the expression of CK20 (**Figure 3C**) and CDX2 (**Figure 3D**) was negative. The area of intraepithelial ductal spread from ICC (**Figure 3E**) showed positive expression of CK7 (**Figure 3F**) and CDX2 (**Figure 3H**), whereas the expression of CK20 (**Figure 3G**) was negative. Another patient had ICC with no evidence of intraepithelial ductal spread along the bile ducts. CT depicted a mass without bile duct dilatation in the anterior section of the liver. The tumor cells of primary ICC showed positive expression of CK7, whereas the expression of CK20, CDX2 and MUC5AC was negative.

DISCUSSION

Intraepithelial ductal spread along the bile ducts may make it difficult to discriminate CRLM from primary biliary neoplasms without knowledge of the clinical details because intraepithelial ductal spread from CRLM closely resembles high-grade dysplasia or carcinoma *in situ* of the bile ducts, as described by Riopel *et al.* (1). Past history of colorectal adenocarcinoma is informative for pathologists to discriminate between CRLM and ICC. Two recent patients with primary ICC who had a past history of surgical resection for colorectal adenocarcinoma prompted the current study based on immunohistochemical analysis, which demonstrated that among the tested immunophenotypes, immunohistochemical combination of CK7 and CK20 for the histological evaluation of intraepithelial ductal spread is useful for discrimination between CRLM and ICC.

Although studies of bile duct involvement in CRLM vary widely with respect to cited incidence from 6.1%-42% (19-24), the incidence of intraepithelial ductal spread from CRLM is unknown (1, 9-12). We found a high incidence of intraepithelial ductal spread along the bile ducts in patients with CRLM with bile duct involvement in the current study, which relied on histological examination of one section only from each tissue block. Our evaluation therefore represented the minimum incidence of intraepithelial ductal spread from CRLM, suggesting that intraepithelial ductal spread along the bile ducts is a common feature of CRLM with bile duct involvement.

CDX2 is a new, highly specific and sensitive marker of the intestinal origin of adenocarcinoma (13). Tot (8) reported that CK20-positive/CK7-negative immunophenotype is more specific in predicting the colorectal origin of liver metastasis than CDX2 expression. In the current series, CDX2-positive/CK7-negative immunophenotype showed higher accuracy (accuracy, 97%) than CK20-positive/CK7-negative immunophenotype (accuracy, 95%) for evaluation of intraepithelial ductal spread from CRLM. However, positive expression of CDX2 was occasionally observed in the areas of intraepithelial ductal spread from ICC (**Table 1** and **Figure 3H**). Furthermore, CK7-positive/CDX2-negative immunophenotype showed lower accuracy (accuracy, 77%) than CK7-positive/CK20-negative immunophenotype (accuracy, 85%) for evaluation of intraepithelial ductal spread from ICC. Taken together, these findings suggest that immunohistochemical combination of CK7 and CK20 for the histological evaluation of intraepithelial ductal spread along the bile ducts allows discrimination between CRLM and ICC.

New effective chemotherapy regimens, such as irinotecan (25, 26), FOLFOX (5-fluorouracil, leucovorin, oxaliplatin) (27), bevacizumab (28) and cetuximab (29) provide survival benefits for patients

with CRLM, whereas cisplatin plus gemcitabine is an appropriate option for the treatment of patients with advanced biliary cancer (30). As the majority of CRLM with bile duct involvement showed intraepithelial ductal spread along the bile ducts, mimicking primary ICC, firm histological diagnosis with knowledge of the clinical details is of importance for making a decision regarding chemotherapy regimen (31). When intraepithelial ductal spread along the bile ducts is found to be positive in the resected specimens, discrimination between intraepithelial ductal spread of CRLM and that of ICC is important. To make a firm histological evaluation of intraepithelial ductal spread along the bile ducts, immunohistochemical combination of CK7 and CK20 appears to be useful for discriminating between CRLM and ICC.

There are two main limitations to the current study. First, it was a retrospective analysis of a small number of patients with intraepithelial ductal spread along the bile ducts. Second, the amount of tested immunophenotypes was limited. To our knowledge, however, this is one of the largest series dealing with intraepithelial ductal spread along the bile ducts of CRLM and that of ICC.

TABLE 1 Immunohistochemical Analysis in Tumor Specimens of Intraepithelial Ductal Spread for Discrimination between CRLM and ICC

Variable	Modality	No. of patients		p value
		CRLM (n=17)	ICC (n=22)	
CK7	Negative	17 (100%)	1 (5%)	<0.001
	Positive	0 (0%)	21 (95%)	
CK20	Negative	1 (6%)	16 (73%)	<0.001
	Positive	16 (94%)	6 (27%)	
CDX2	Negative	0 (0%)	13 (59%)	<0.001
	Positive	17 (100%)	9 (41%)	
MUC2	Negative	8 (47%)	14 (64%)	0.345
	Positive	9 (53%)	8 (36%)	
MUC5AC	Negative	15 (88%)	4 (18%)	<0.001
	Positive	2 (12%)	18 (82%)	
HGM	Negative	14 (82%)	4 (18%)	<0.001
	Positive	3 (18%)	18 (82%)	

CRLM: colorectal carcinoma liver metastasis; ICC: intrahepatic cholangiocarcinoma; HGM: human gastric mucin

CONCLUSIONS

Intraepithelial ductal spread along the bile ducts is a common feature of CRLM with bile duct involvement. Among the tested immunophenotypes, immunohistochemical combination of CK7 and CK20 for the histological evaluation of intraepithelial ductal spread is useful for discrimination between CRLM and ICC.

REFERENCES

1. **Riopel MA, Klimstra DS, Godellas CV, Blumgart LH, Westra WH:** Intrabiliary growth of metastatic colonic adenocarcinoma: a pattern of intrahepatic spread easily confused with primary neoplasia of the biliary tract. Am J Surg Pathol 1997; 21:1030-1036.
2. **Maeda T, Kajiyama K, Adachi E, Takenaka K, Sugimachi K, Tsuneyoshi M:** The expression of cytokeratins 7, 19, and 20 in primary and metastatic carcinomas of the liver. Mod Pathol 1996; 9:901-909.
3. **Tot T:** Adenocarcinomas metastatic to the liver: the value of cytokeratins 20 and 7 in the search for unknown primary tumors. Cancer 1999; 85:171-177.
4. **Rullier A, Le Bail B, Fawaz R, Blanc JF, Saric J, Bioulac-Sage P:** Cytokeratin 7 and 20 expression in cholangiocarcinomas varies along the biliary tract but still differs from that in colorectal carcinoma metastasis. Am J Surg Pathol 2000; 24:870-876.
5. **Shimonishi T, Miyazaki K, Nakanuma Y:** Cytokeratin profile relates to histological subtypes and intrahepatic location of intrahepatic cholangiocarcinoma and primary sites of metastatic adenocarcinoma of liver. Histopathology 2000; 37:55-63.
6. **Chu P, Wu E, Weiss LM:** Cytokeratin 7 and cytokeratin 20 expression in epithelial neoplasms: a survey of 435 cases. Mod Pathol 2000; 13:962-972.
7. **Tot T:** Cytokeratins 20 and 7 as biomarkers: usefulness in discriminating primary from metastatic adenocarcinoma. Eur J Cancer 2002; 38:758-763.
8. **Tot T:** Identifying colorectal metastases in liver biopsies: the novel CDX2 antibody is less specific than the cytokeratin 20+/7- phenotype. Med Sci Monit 2004; 10:BR139-143.
9. **Uehara K, Hasegawa H, Ogiso S, et al:** Intrabiliary polypoid growth of liver metastasis from colonic adenocarcinoma with minimal invasion of the liver parenchyma. J Gastroenterol 2004; 39:72-75.
10. **Takamatsu S, Teramoto K, Kawamura T, et al:** Liver metastasis from rectal cancer with prominent intrabile duct growth. Pathol Int 2004; 54:440-445.
11. **Itatsu K, Fujii T, Sasaki M, Zen Y, Nakanuma Y:** Intraductal papillary cholangiocarcinoma and atypical biliary epithelial lesions confused with intrabiliary extension of metastatic colorectal carcinoma. Hepatogastroenterology 2007; 54:677-680.
12. **Kayashima H, Taketomi A, Yamashita Y, et al:** Liver metastasis with intraductal invasion originating from rectal cancer: report of a case. Surg Today 2008; 38:765-768.
13. **Kaimaktchiev V, Terracciano L, Tornillo L, et al:** The homeobox intestinal differentiation factor CDX2 is selectively expressed in gastrointestinal adenocarcinomas. Mod Pathol 2004; 17:1392-1399.
14. **Zen Y, Sasaki M, Fujii T, et al:** Different expression patterns of mucin core proteins and cytokeratins during intrahepatic cholangiocarcinogenesis from biliary intraepithelial neoplasia and intraductal papillary neoplasm of the bile duct--an immunohistochemical study of 110 cases of hepatolithiasis. J Hepatol 2006; 44:350-358.
15. **Aishima S, Kuroda Y, Nishihara Y, et al:** Gastric mucin phenotype defines tumour progression and prognosis of intrahepatic cholangiocarcinoma: gastric foveolar type is associated with aggressive tumour behaviour. Histopathology 2006; 49:35-44.
16. **Krasinskas AM, Goldsmith JD:** Immunohistology of the Gastrointestinal Tract. In: Dabbs DJ (ed). Diagnostic Immunohistochemistry, 3rd edn. Philadelphia, Pennsylvania: Saunders Elsevier, 2010: 500-540.
17. **Nagata S, Ajioka Y, Nishikura K, et al:** Co-expression of gastric and biliary phenotype in pyloric-gland type adenoma of the gallbladder: immunohistochemical analysis of mucin profile and CD10. Oncol Rep 2007; 17:721-729.

18. **Shiroshita H, Watanabe H, Ajioka Y, Watanabe G, Nishikura K, Kitano S:** Re-evaluation of mucin phenotypes of gastric minute well-differentiated-type adenocarcinomas using a series of HGM, MUC5AC, MUC6, M-GGMC, MUC2 and CD10 stains. Pathol Int 2004; 54:311-321.
19. **Yasui K, Hirai T, Kato T, et al:** A new macroscopic classification predicts prognosis for patient with liver metastases from colorectal cancer. Ann Surg 1997; 226:582-586.
20. **Sasaki A, Aramaki M, Kawano K, Yasuda K, Inomata M, Kitano S:** Prognostic significance of intrahepatic lymphatic invasion in patients with hepatic resection due to metastases from colorectal carcinoma. Cancer 2002; 95:105-111.
21. **Minagawa M, Makuuchi M, Torzilli G, et al:** Extension of the frontiers of surgical indications in the treatment of liver metastases from colorectal cancer: long-term results. Ann Surg 2000; 231:487-499.
22. **Okano K, Yamamoto J, Moriya Y, et al:** Macroscopic intrabiliary growth of liver metastases from colorectal cancer. Surgery 1999; 126:829-834.
23. **Korita PV, Wakai T, Shirai Y, et al:** Intrahepatic lymphatic invasion independently predicts poor survival and recurrences after hepatectomy in patients with colorectal carcinoma liver metastases. Ann. Surg. Oncol. 2007; 14:3472-3480.
24. **Wakai T, Shirai Y, Sakata J, et al:** Appraisal of 1 cm hepatectomy margins for intrahepatic micrometastases in patients with colorectal carcinoma liver metastasis. Ann Surg Oncol 2008; 15:2472-2481.
25. **Saltz LB, Cox JV, Blanke C, et al:** Irinotecan plus fluorouracil and leucovorin for metastatic colorectal cancer. Irinotecan Study Group. N Engl J Med 2000; 343:905-914.
26. **Mackay HJ, Billingsley K, Gallinger S, et al:** A multicenter phase II study of "adjuvant" irinotecan following resection of colorectal hepatic metastases. Am J Clin Oncol 2005; 28:547-554.
27. **Nordlinger B, Sorbye H, Glimelius B, et al:** Perioperative chemotherapy with FOLFOX4 and surgery versus surgery alone for resectable liver metastases from colorectal cancer (EORTC Intergroup trial 40983): a randomised controlled trial. Lancet 2008; 371:1007-1016.
28. **Hurwitz H, Fehrenbacher L, Novotny W, et al:** Bevacizumab plus irinotecan, fluorouracil, and leucovorin for metastatic colorectal cancer. N Engl J Med 2004; 350:2335-2342.
29. **Cunningham D, Humblet Y, Siena S, et al:** Cetuximab monotherapy and cetuximab plus irinotecan in irinotecan-refractory metastatic colorectal cancer. N Engl J Med 2004; 351:337-345.
30. **Valle J, Wasan H, Palmer DH, et al:** Cisplatin plus gemcitabine versus gemcitabine for biliary tract cancer. N Engl J Med 2010; 362:1273-1281.
31. **Varadhachary GR, Raber MN, Matamoros A, Abbruzzese JL:** Carcinoma of unknown primary with a colon-cancer profile-changing paradigm and emerging definitions. Lancet Oncol 2008; 9:596-599.

Cancer Science
The official journal of the Japanese Cancer Association JCA

Phase I study of TAC-101, an oral synthetic retinoid, in Japanese patients with advanced hepatocellular carcinoma

Takuji Okusaka,[1,3] Hideki Ueno,[1] Masafumi Ikeda,[2] Yoriko Takezako[1] and Chigusa Morizane[1]

[1]Hepatobiliary and Pancreatic Oncology Division, National Cancer Center Hospital, Tokyo; [2]Division of Hepatobiliary and Pancreatic Oncology, National Cancer Center Hospital East, Kashiwa, Chiba, Japan

(Received February 14, 2012/Revised May 6, 2012/Accepted May 8, 2012/Accepted manuscript online May 16, 2012/Article first published online June 18, 2012)

Preclinical models have shown that TAC-101 (4-[3,5-bis(trimethylsilyl) benzamide] benzoic acid), an oral synthetic retinoid, has antitumor activity in hepatocellular carcinoma (HCC). We conducted a phase I study in Japanese patients with advanced HCC to examine the pharmacokinetics, recommended dose, safety, and efficacy of TAC-101. The administered dose of TAC-101 was 10 mg/day in four patients (level 1), 20 mg/day in six (level 2), and 30 mg/day in three (level 3). There was no dose-limiting toxicity at level 1. Only one patient each had dose-limiting toxicity at level 2 (grade 2 fatigue, recovery requiring eight or more consecutive days of rest) and at level 3 (grade 3 splenic vein thrombosis). Level 3 (30 mg/day) was considered the maximum tolerated dose and 20 mg/day the recommended dose by a panel of medical experts, placing maximum emphasis on safety. The most frequent adverse events were fatigue, headache, and dermal symptoms such as rash. Pharmacokinetic parameters in Japanese patients with HCC were similar to those in patients in the United States, most of whom were Caucasian. Although no patient had a complete or partial response, the disease control rate was 38.5%. In conclusion, the recommended dose of TAC-101 for patients with HCC is 20 mg/day. TAC-101 had an acceptable toxicity profile, warranting further evaluation in clinical trials. (*Cancer Sci* 2012; 103: 1524–1530)

Hepatocellular carcinoma (HCC) is one of the most common cancers in the world. Outcomes remain poor because disease is usually advanced at diagnosis and associated with hepatic impairment and a high rate of recurrence, resulting from either intrahepatic metastases from the primary tumor or multicentric lesions. Surgical resection, liver transplantation, radiofrequency ablation (RFA) or percutaneous ethanol injection (PEI) are the mainstays of treatment in patients with potentially curable disease. Transcatheter arterial chemoembolization (TACE) is the procedure of choice for noncurative HCC. Currently marketed systemic chemotherapeutic agents, with the exception of sorafenib, provide only marginal benefits.[1–3] Despite the survival benefit demonstrated for sorafenib, more effective systemic therapy for HCC is required.

TAC-101 (4-[3,5-bis(trimethylsilyl) benzamido] benzoic acid) is an orally absorbed synthetic retinoid. This analogue of vitamin A (retinol) binds to nuclear retinoic acid receptor-α (RAR-α), activates RAR-α transcriptional activity, and has shown antitumor activity in primary and metastatic preclinical models of liver cancer.[4,5] TAC-101 inhibits tumor growth in the liver with low toxicity and markedly improves survival in both primary HCC and metastatic colon cancer models.[6]

In the United States, an initial dose-escalation study was performed in patients with advanced cancer. TAC-101 was orally administered daily, without a rest period. The most frequent toxicities were skin and mucosal membrane disorders, myalgia/arthralgia, fatigue, and triglyceridemia. Dose-limiting toxicities (DLT) occurring during the first 28 days of treatment (cycle 1) were fatigue, arthralgia/joint pain, myalgia, and venous thromboembolism (VTE). VTE developed in nine of 29 patients as a characteristic adverse reaction of TAC-101; the dose ranged from 12 to 34 mg/m^2.[7] In a phase I/II study, TAC-101 was administered orally in 21-day cycles (14 days on/7 days off) to patients with advanced HCC. In the phase I portion of the study, the initial dose was 40 mg/day. Two patients had DLT, and the dose was reduced to 20 mg/day. Since only 1 of 6 assessable patients had DLT during the first two cycles of therapy, 20 mg/day was designated as the maximum tolerated dose (MTD) for the 21-day treatment cycle. At this dose level, TAC-101 was generally well tolerated, and the most common drug-related adverse events were increased blood triglyceride levels, fatigue, dermatitis, pruritus, nausea, dry skin, myalgias, dry mouth, arthralgias, anorexia, diarrhea, and headache. Among 21 evaluable patients, no patient had a complete response (CR) or partial response (PR), but 12 (57%) had stable disease (SD). Median progression free survival (PFS) and overall survival (OS) were 3.4 months and 19.2 months, respectively.[8]

We report the results of the first phase I study of TAC-101 in Japanese patients with HCC. Our major goals were to evaluate safe dose levels, tolerability, pharmacokinetics, and efficacy.

Materials and Methods

Eligibility. Eligible patients had pathologically or clinically proved advanced HCC that was not amenable to standard treatments. A hypervascular mass on diagnostic imaging was considered a sufficient non-invasive diagnostic criterion for HCC. At least one measurable lesion on CT or MRI (not including necrotic lesions caused by prior treatment) was required. Other eligibility criteria included an age of 20 to 75 years; an Eastern Cooperative Oncology Group (ECOG) performance status (PS) of 0 to 2; an estimated life expectancy of at least 60 days; adequate hematologic function (white blood cell [WBC] $\geq 3000/mm^3$, hemoglobin ≥ 8.0 g/dL, platelets $\geq 5.0 \times 10^4/mm^3$); adequate hepatic function (aspartate aminotransferase [AST] and alanine aminotransferase [ALT] ≤ 5 times the upper limit of normal [ULN], total bilirubin ≤ 2.0 mg/dL, serum albumin ≥ 2.8 g/dL, and prothrombin activity $\geq 40\%$); adequate renal function (serum creatinine

[3]To whom correspondence should be addressed.
E-mail: tokusaka@ncc.go.jp
Clinical trial registration: This trial was not registered in the clinical trial database because it was an early phase trial and not a controlled study.

doi: 10.1111/j.1349-7006.2012.02334.x

Table 1. Summary of patient background characteristics

Background characteristics		10 mg/day	20 mg/day	30 mg/day	Total (%)
No. eligible patients		*n* = 4	*n* = 6	*n* = 3	*n* = 13
Gender	Male	3	5	3	11 (84.6)
	Female	1	1	0	2 (15.4)
Age (years)	<65	2	0	2	4 (30.8)
	≥65	2	6	1	9 (69.2)
	Median	64	72	60	70
	Min., Max.	59, 70	66, 74	45, 70	45, 74
ECOG, PS	0	4	5	3	12 (92.3)
	1	0	1	0	1 (7.7)
Stage*	Stage I	0	0	0	0 (0.0)
	Stage II	1	1	0	2 (15.4)
	Stage III	2	4	2	8 (61.5)
	Stage IVA	0	0	0	0 (0.0)
	Stage IVB	1	1	1	3 (23.1)
Child–Pugh classification	A	3	2	3	8 (61.5)
	B	1	4	0	5 (38.5)
	C	0	0	0	0 (0.0)
Grade of histological differentiation	Well differentiated	2	1	0	3 (23.1)
	Moderately differentiated	0	3	1	4 (30.8)
	Poorly differentiated	0	0	1	1 (7.7)
	Unknown	2	2	1	5 (38.5)
Extrahepatic metastasis	No	3	5	2	10 (76.9)
	Yes	1	1	1	3 (23.1)
History of hepatectomy	No	1	3	2	6 (46.2)
	Yes	3	3	1	7 (53.8)
History of nonsurgical therapy	No	0	0	0	0 (0.0)
	Yes	4	6	3	13 (100.0)

*According to the staging system of the Liver Cancer Study Group of Japan (4th edition). ECOG, PS Eastern Cooperative Oncology Group performance status.

≤1.5 times the ULN); and a Child–Pugh class of A or B. Resection was permitted if the procedure had been performed at least 180 days before registration in the study. Other prior treatments for HCC were permitted if such treatment had been performed at least 30 days before registration. Patients were excluded if they had tumors involving more than 50% of the liver; brain or bone metastases or vascular invasion of the main trunk and first branch(es) of the portal vein, the main trunk of the left/middle/right hepatic veins, the inferior right hepatic vein, the short hepatic veins, or the inferior vena cava; severe complications; other malignancies; or inability to comply with the protocol requirements. Patients were also excluded if they had a history of VTE. Patients who were receiving anticoagulants or hormone replacement therapy were excluded. Written informed consent was obtained from each patient. The study was approved by the local institutional review boards of the National Cancer Center Hospital, Japan.

Study design and treatment plan. TAC-101 was supplied by Taiho Pharmaceutical Co., Ltd. (Tokyo, Japan). This study evaluated the pharmacokinetics of TAC-101 and established the MTD for two courses of treatment. Patients received the assigned dose of TAC-101 once daily (after breakfast) for 14 consecutive days, followed by a 7-day rest (a 21-day treatment course). If grade 3 or higher hematologic toxicity or grade 2 or higher nonhematologic toxicity occurred, the dose of TAC-101 could be reduced (minimum dose, 10 mg/day). If DLT occurred, treatment with TAC-101 could be temporarily suspended. Treatment was continued until evidence of disease progression. Treatment was terminated if recovery from an adverse event required more than 21 days, if the patient requested treatment to be discontinued, or if unacceptable toxicity developed in the opinion of the investigator.

The starting dose of TAC-101 (level 1) was 10 mg/day, level 2 was 20 mg/day, level 3 was 30 mg/day, level 4 was 40 mg/day, level 5 was 50 mg/day, and level 6 was 60 mg/day. Patients were enrolled in cohorts of three for each dose level. The dose was escalated according to cohort and was not increased in the same patient. If none of the first three patients had DLT during the first two cycles of therapy, the dose was increased to the next dose level. If one or two of the first three patients had DLT, three additional patients were assigned to the same dose level; if only one or two of the first six patients had DLT, the dose was increased to the next dose level; if all of the first three patients or three or more of the first six patients had DLT, the dose was defined as the MTD; the recommended dose (RD) was defined as the level one step below the MTD. A total of six patients received the RD to confirm the safety profile. DLT was defined as any of the following: (i) hematologic toxicity ≥Grade 4; (ii) nonhematologic toxicity ≥Grade 3; (iii) AST, ALT ≥10 times the ULN; or (iv) a rest period of eight or more consecutive days was required.

Pharmacokinetics. Blood samples for pharmacokinetic analysis were collected before and 2, 4, 6, 8, 10 to 12, and 24 h after administration of TAC-101 on day 1 and after repeated treatment (days 8–13) during the first cycle (approximately 4 mL for each time point). The blood samples were centrifuged, and the resulting plasma samples were stored at −20°C until analysis. Spontaneously voided urine was collected before treatment on day 1 (baseline urine), from 0 to 8 h after treatment (0–8 h pooled urine), and from 8 to 24 h after treatment (8–24 h pooled urine). The urine samples were stored at −20°C until analysis.

Plasma concentrations of TAC-101 were measured using a validated method. The analyte was extracted with *tert*-butyl methyl ether and analyzed by liquid chromatography/tandem mass spectrometry (LC/MS/MS; Waters 2690/Finnigan MAT TSQ7000) with negative ion-electrospray ionization mode, using deuterium-labeled TAC-101 as an internal standard.

Pharmacokinetic parameters were calculated from the plasma concentrations of TAC-101 by non-compartmental analysis using WinNonlin software, version 4.1 (Pharsight, Cary, NC, USA).

For both plasma and urine samples, the metabolites of TAC-101 were preliminarily analyzed using an ultraviolet detector-equipped, high-performance liquid chromatograph and LC/MS/MS (Agilent 1100 series/Applied Biosystems API 4000, Carlsbad, CA, USA). The metabolites TAC-101-M-1, TAC-101-M-2, and TAC-101-M-3 were identified by comparison with authentic samples synthesized by Taiho Pharmaceuticals (Tokyo, Japan). The structures of conjugates were estimated by analyzing the mass fragmentation spectra. Concentrations of TAC-101-M-1 and TAC-101-M-2 were determined using an LC/MS/MS method similar to that used for the assay of TAC-101.

Assessment of efficacy and toxicity. All eligible patients who received at least one dose of the study drug were included in the evaluations of response and toxicity. The criteria of the Japan Society of Clinical Oncology, which closely resemble the World Health Organization criteria, were used to evaluate unblended radiographic tumor responses at the study site. Computed tomography or MRI was used to evaluate measurable disease; the same imaging modality was used at baseline and follow-up. The efficacy endpoints were the overall response rate, the duration of antitumor effect, OS, time to progression (TTP), and time to treatment failure (TTF). Vital signs, physical findings, and the results of hematological and biochemical testing, including thrombosis panel and urine analyses, were assessed at 2-week intervals during treatment and after the 7-day recovery period. The severities of all adverse events were evaluated according to the National Cancer Institute Common Toxicity Criteria, version 2.0 (NCI-CTC Ver. 2.0). The durations of all adverse events and their relations to TAC-101 were initially assessed by the attending physicians. Subsequently, an independent review committee reassessed data on adverse events and evaluated the radiologic tumor responses in a blinded manner using Response Evaluation Criteria in Solid Tumors (RECIST).[9]

Statistical considerations. All data were summarized using descriptive statistics for continuous variables and frequencies and percentages for discrete variables. Median times to events were estimated using the Kaplan–Meier method.

Results

Patient characteristics and treatment. Between October 2003 and May 2005, a total of 13 patients were enrolled at a single site in Japan. All patients were eligible for the evaluation of toxicity and efficacy. The first four patients received dose level 1 (10 mg/day), the next six patients received dose level 2 (20 mg/day), and the last three patients received dose level 3 (30 mg/day). The characteristics of the patients are summarized in Table 1. At study entry, three (23.1%) of the 13 patients had metastatic disease. All 13 patients had received some prior treatment, including one previously given systemic chemotherapy with the oral fluoropyrimidine tegafur-uracil (UFT).

Dose-limiting toxicity and recommended dose. One of the first three patients assigned to level 1 (10 mg/day) discontinued the study medication before completing two courses of treatment because of non-drug-related serious adverse events mentioned in the section of adverse events. Therefore, another patient was assigned to this level, and safety was evaluated in a total of four patients. Because no DLT occurred at this level, the dose was increased to level 2 (20 mg/day). One of the first three patients given level 2 had DLT, and three patients were additionally assigned to this dose level; safety was thus

Table 2. Drug-related adverse events with incidence ≥20% or grade 3–4

Drug-related adverse event	10 mg/day (n = 4)		20 mg/day (n = 6)		30 mg/day (n = 3)		Child–Pugh A (n = 8)		Child–Pugh B (n = 5)		Total (n = 13)	
	All grade (%)	Grade ≥ 3 (%)	All grade (%)	Grade ≥ 3 (%)	All grade (%)	Grade ≥ 3 (%)	All grade (%)	Grade ≥ 3 (%)	All grade (%)	Grade ≥ 3 (%)	All grade (%)	Grade ≥ 3 (%)
Splenic vein thrombosis	0 (0)	0 (0)	0 (0)	0 (0)	1 (33)	1 (33)	1 (13)	1 (13)	0 (0)	0 (0)	1 (8)	1 (8)
Headache	4 (100)	0 (0)	2 (33)	0 (0)	1 (33)	0 (0)	5 (63)	0 (0)	2 (40)	0 (0)	7 (54)	0 (0)
Cough	1 (25)	0 (0)	5 (83)	0 (0)	0 (0)	0 (0)	2 (25)	0 (0)	4 (80)	0 (0)	6 (46)	0 (0)
Rhinorrhea	1 (25)	0 (0)	3 (50)	0 (0)	0 (0)	0 (0)	1 (13)	0 (0)	3 (60)	0 (0)	4 (31)	0 (0)
Alopecia	1 (25)	0 (0)	2 (33)	0 (0)	1 (33)	0 (0)	2 (25)	0 (0)	2 (40)	0 (0)	4 (31)	0 (0)
Eczema	1 (25)	0 (0)	3 (50)	0 (0)	0 (0)	0 (0)	2 (25)	0 (0)	2 (40)	0 (0)	4 (31)	0 (0)
Rash	3 (75)	0 (0)	1 (17)	0 (0)	3 (100)	0 (0)	6 (75)	0 (0)	1 (20)	0 (0)	7 (54)	0 (0)
Arthralgia	1 (25)	0 (0)	3 (50)	0 (0)	1 (33)	0 (0)	3 (38)	0 (0)	2 (40)	0 (0)	5 (39)	0 (0)
Myalgia	2 (50)	0 (0)	0 (0)	0 (0)	1 (33)	0 (0)	3 (38)	0 (0)	0 (0)	0 (0)	3 (23)	0 (0)
Fatigue	1 (25)	0 (0)	4 (67)	0 (0)	1 (33)	0 (0)	3 (38)	0 (0)	3 (60)	0 (0)	6 (46)	0 (0)
Blood cholesterol increased	1 (25)	0 (0)	0 (0)	0 (0)	3 (100)	0 (0)	4 (50)	0 (0)	0 (0)	0 (0)	4 (31)	0 (0)
Blood lactate dehydrogenase increased	1 (25)	0 (0)	1 (17)	0 (0)	3 (100)	0 (0)	4 (50)	0 (0)	1 (20)	0 (0)	5 (39)	0 (0)
Blood triglycerides increased	3 (75)	0 (0)	4 (67)	0 (0)	3 (100)	0 (0)	7 (88)	0 (0)	3 (60)	0 (0)	10 (77)	0 (0)
Fibrin D dimer increased	2 (50)	0 (0)	6 (100)	0 (0)	3 (100)	0 (0)	6 (75)	0 (0)	5 (100)	0 (0)	11 (85)	0 (0)
Thrombin-antithrombin III complex increased	1 (25)	0 (0)	5 (83)	0 (0)	3 (100)	0 (0)	6 (75)	0 (0)	3 (60)	0 (0)	9 (69)	0 (0)
Blood alkaline phosphatase increased	2 (50)	0 (0)	1 (17)	0 (0)	1 (33)	0 (0)	3 (38)	0 (0)	1 (20)	0 (0)	4 (31)	0 (0)

The worst grade was used to calculate the incidence according to grade.

doi: 10.1111/j.1349-7006.2012.02334.x

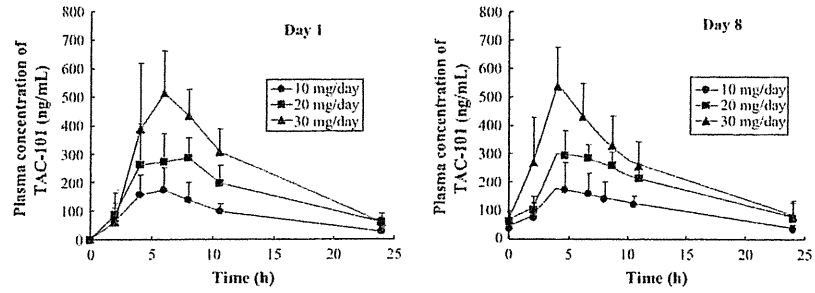

Fig. 1. Plasma concentration-time profile of TAC-101 (4-[3,5-bis(trimethylsilyl) benzamide] benzoic acid) in patients with hepatocellular carcinoma.

Table 3. Pharmacokinetic values of TAC-101 in patients with hepatocellular carcinoma

Blood sampling day	PK parameter	10 mg/day			20 mg/day			30 mg/day		
		No. patients	Mean	SD	No. patients	Mean	SD	No. patients	Mean	SD
Day 1	C_{max} (ng/mL)	4	189.2	85.5	6	333.0	88.6	3	512.1	149.5
	t_{max} (h)	4	5.5	1.0	6	5.7	2.0	3	6.0	0.0
	AUC_{0-24} (ng h/mL)	4	2084	640	6	3900	1140	3	5780	1489
	AUC_{inf} (ng h/mL)	3	2526	497	4	4680	1657	3	6261	1596
	$t_{1/2}$ (h)	3	5.54	0.75	4	6.92	1.67	3	5.57	0.57
	Vd/F (L)	3	32.2	5.6	4	45.5	12.7	3	39.9	9.6
	CL/F (L/h)	3	4.08	0.89	4	4.83	2.15	3	4.98	1.11
Day 8	C_{max} (ng/mL)	4	207.7	71.0	6	326.0	66.9	3	543.9	138.9
	t_{max} (h)	4	6.0	2.9	6	5.7	2.0	3	4.0	0.0
	AUC_{0-24} (ng h/mL)	4	2401	630	6	4191	1063	3	6099	1772
	AUC_{inf} (ng h/mL)	3	2906	755	4	4674	820	3	7257	2410
	$t_{1/2}$ (h)	3	6.47	0.92	4	7.50	0.97	3	8.16	3.59
	Vd/F (L)	3	32.9	5.1	4	46.9	6.4	3	49.3	13.9
	CL/F (L/h)	3	3.62	1.05	4	4.39	0.81	3	4.55	1.87

AUC_{inf}, area under the plasma concentration-time curve up to infinity; AUC_{0-24}, area under the plasma concentration-time curve up to 24 h post-dose; CL/F, oral clearance; C_{max}, maximum plasma concentration; SD, standard deviation; t_{max}, time of maximum concentration; $t_{1/2}$, elimination half-life; Vd/F, apparent volume of distribution.

assessed in a total of six patients. The DLT was grade 2 fatigue requiring eight or more consecutive days of rest for recovery. Because no other patient had DLT, the dose level was increased to level 3 (30 mg/day). Splenic vein thrombosis, a grade 3 drug-related adverse event, occurred in one patient at this level. Although only one patient given 30 mg/day of the study drug had DLT, this dose level was designated as the MTD and 20 mg/day as the RD by a panel of medical experts on an independent monitoring committee, who considered the thromboembolic event to be of great importance on the basis of the results of studies conducted in the United States, in which the event developed in nine of 29 patients and was potentially fatal.

Treatment delivered. Four patients received a total of 14 cycles of treatment at 10 mg/day (median, three cycles per patient; range, 1–7). Six patients received a total of 21 cycles of treatment at 20 mg/day (median, three cycles per patient; range, 2–8). Three patients received a total of seven cycles of treatment at 30 mg/day (median, three cycles per patient; range, 2–3). The dose of TAC-101 was not reduced in any patient. The reasons for terminating treatment were progressive disease in nine patients (69.2%), adverse events in two (15.4%), and other reasons in two (15.4%; one required 21 or more consecutive days of rest, and one withdrew consent).

Adverse events. Drug-related adverse events occurring in the 13 patients are shown in Table 2. Treatment with TAC-101 was generally well tolerated throughout the study. Grade 3 or 4 toxicity (splenic vein thrombosis) occurred in only one patient, who received 30 mg/day of TAC-101. The patient was a 70-year-old, HCV-positive man with Child–Pugh A liver cirrhosis, hypersplenism, and hypertension. He had multiple tumors smaller than 3 cm in diameter in the liver, without vascular invasion or extrahepatic metastasis. Splenic vein thrombosis was noted during a routine restaging CT scan of the target lesion at the end of the third course of therapy. The patient received aspirin, and the thrombosis was considered resolved 85 days after the initiation of treatment with aspirin. The most common toxic effects were fibrin D dimer increased (84.6%), blood triglycerides increased (76.9%), thrombin-antithrombin III complex increased (69.2%), headache and rash (53.8%). Serious adverse events were anorexia, hepatic encephalopathy, renal disorder, aspiration pneumonia, and sepsis in one patient who received 10 mg/day. These events were considered unrelated to the study medication. As for differences in drug-related adverse events between the Child–Pugh A and B groups, the incidences of some events were at least 20 percentage points higher in the Child–Pugh B group than in the Child–Pugh A group, such as cough (25% *vs* 80%), rhinorrhea (13% *vs* 60%), fatigue (38% *vs* 60%), and fibrin D dimer increased (75% *vs* 100%). However, the incidences and severities of most other events were similar in the two groups.

Efficacy. Response could be evaluated in all 13 patients. No patient had a CR or PR. A total of nine patients (69.2%, 9/13) had no change (NC): two of four patients at 10 mg/day, five of six at 20 mg/day, and two of three at 30 mg/day. Four

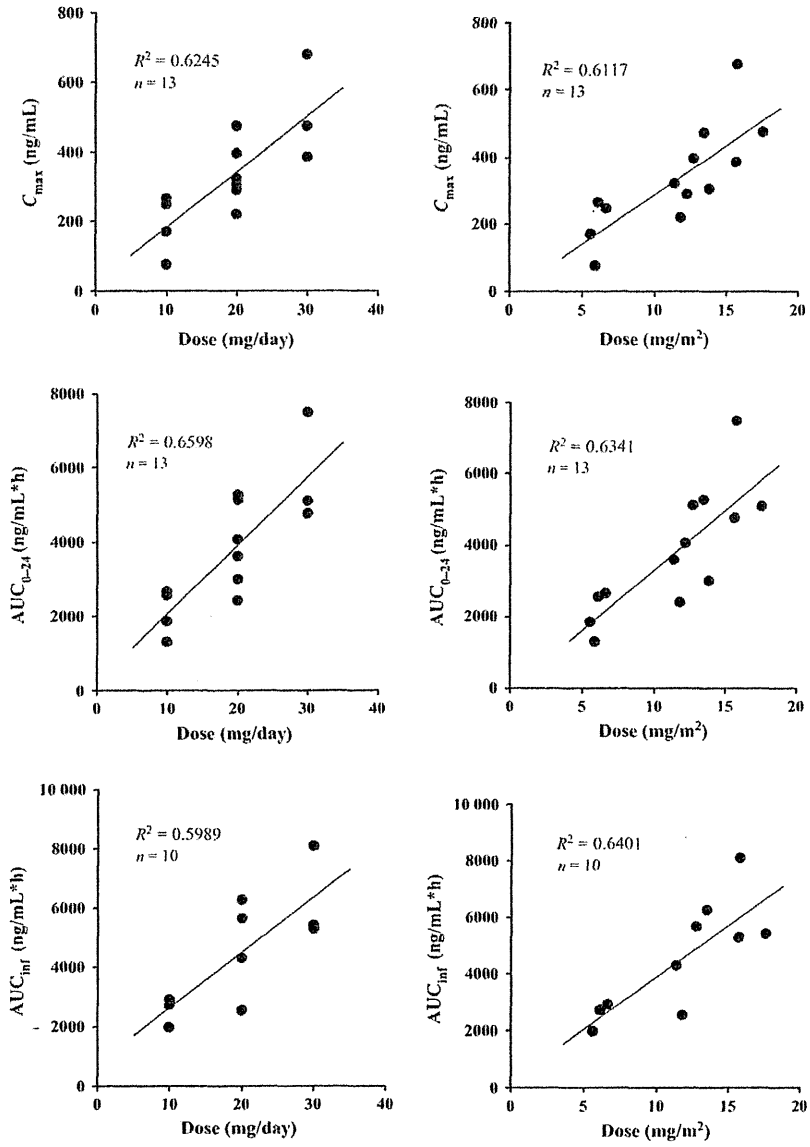

Fig. 2. Relation between TAC-101 (4-[3,5-bis(trimethylsilyl) benzamide] benzoic acid) dose and C_{max} or AUC in patients with hepatocellular carcinoma on day 1 (single dose). The x axes of the left- and right-hand figures represent the dose per day and dose per m^2, respectively.

patients (30.8%, 4/13) had progressive disease (PD): two of four at 10 mg/day, one of six at 20 mg/day, and one of three at 30 mg/day. No change was maintained for 8 weeks (56 days) or longer (long-term NC) in five patients, and the disease control rate (CR + PR + long-term NC) was thus 38.5% (5/13 patients). Median TTF was 60.0 days (95% CI, 46.0-65.0). Median TTP and OS were 86.0 days (95% CI, 58.0 –146.0) and 427.0 days (95% CI, 369.0-unknown), respectively. When response was evaluated according to RECIST, none of the 13 patients had a PR or CR, 7 (53.8%) had SD, and five (38.5%) had PD.

Pharmacokinetic analysis. Mean plasma concentration-time profiles after administration of TAC-101 on day 1 and on day 8 are shown in Figure 1. The calculated pharmacokinetic parameters of TAC-101 are summarized in Table 3. TAC-101 concentrations in plasma reached peak values approximately 6 h after administration and declined with a half-life ($t_{1/2}$) of 5 –8 h. Consistent with the relatively short $t_{1/2}$, increased plasma concentrations after multiple doses of TAC-101 once daily were not apparent. The relations between the dose of TAC-101 and the maximum plasma concentration (C_{max}), area under the plasma concentration-time curve up to 24 h post-dose (AUC_{0-24}), and area under the plasma concentration-time curve up to infinity (AUC_{inf}) after a single dose (day 1) are shown in Figure 2. These variables generally increased proportionally to the dose of TAC-101 (10–30 mg/day). The relation between the dose of TAC-101 and pharmacokinetic parameters was generally unchanged after adjusting the dose according to individual body surface area. The $t_{1/2}$ of 5.54 to 6.92 h, the apparent volume of distribution (Vd/F) of 32.2 to 45.5 L, and the oral clearance (CL/F) of 4.08 to 4.98 L/h after a single dose of TAC-101 did not differ among the dose levels. All pharmacokinetic parameters were generally similar after a single dose and after repeated doses of TAC-101, suggesting that repeated treatment was not

doi: 10.1111/j.1349-7006.2012.02334.x

associated with changes in TAC-101 metabolism or with drug accumulation.

In this clinical study, a total five patients with Child–Pugh class B disease were enrolled, but the oral clearance of TAC-101 was available for only three of the five patients at the dose level of 20 mg/day. The calculated oral clearance of TAC-101 ranged from 3.44 to 5.67 L/h in patients with Child–Pugh class A disease (n = 7, 10–30 mg/day) and from 3.19 to 7.92 L/h in those with Child–Pugh class B disease (n = 3, 20 mg/day). Although there was no apparent difference in oral clearance between the two groups, firm conclusions were precluded by the limited number of patients in this study.

The pooled plasma and urine samples were analyzed to characterize the metabolites of TAC-101. After a single dose of TAC-101, the hydroxylated metabolites TAC-101-M-1 and TAC-101-M-2 were simultaneously detected in plasma samples along with parent TAC-101. The concentrations of TAC-101-M-1 and TAC-101-M-2 in plasma as determined by LC/MS/MS were approximately 16% and 11% of the concentration of unchanged TAC-101 6 h after treatment and approximately 23% and 16% of the concentration of unchanged TAC-101 10.6 h after treatment (mean sampling time; range, 10–12 h), respectively. The respective percentages on day 8 were comparable to those after the initial dose. These results indicate that the majority of absorbed TAC-101 circulates in the body as a parent drug, with minor proportions of metabolites. In urine samples, the hydroxylated metabolite TAC-101-M-3 and the glucuronide conjugates of TAC-101-M-1 and TAC-101-M-2 were detected. The parent drug TAC-101 was not detected in urine, suggesting that hepatic metabolism is the major elimination pathway of TAC-101, which underwent hydroxylation or glucuronide conjugation, followed by partial excretion of metabolites into urine. Based on these exploratory analyses of human plasma and urine, the metabolic pathways of TAC-101 were determined as shown in Figure 3.

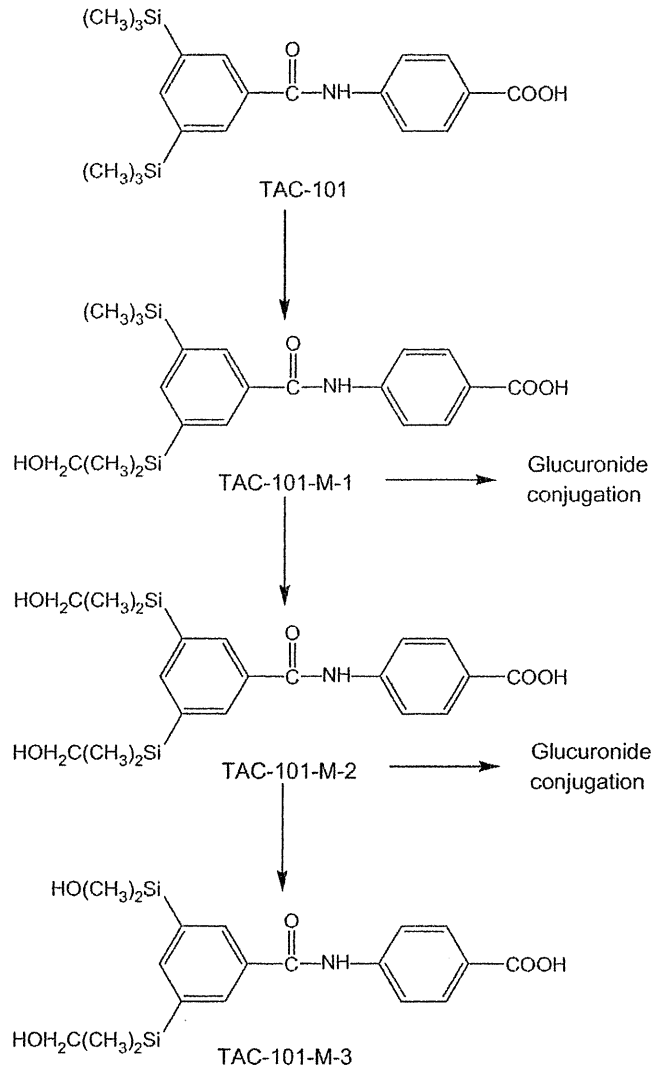

Fig. 3. Metabolic pathways of TAC-101 (4-[3,5-bis(trimethylsilyl) benzamide] benzoic acid) and its metabolites.

Discussion

In one patient given 30 mg/day, CT revealed splenic vein thrombosis, which was considered DLT. Although DLT developed in only one patient receiving 30 mg/day of TAC-101, this dose level was judged to be the MTD by a panel of medical experts who placed maximum emphasis on safety. Mechanisms that potentially trigger thromboembolic events have been studied, but the role of TAC-101 in such events remains unclear.

The most common treatment-related adverse events were fatigue, headache, and dermal symptoms such as rash. However, most adverse events were mild (grade 1 or 2), confirming that TAC-101 is well tolerated at the recommended dose of 20 mg/day. DLT comprised grade 2 fatigue in one patient given 20 mg/day and grade 3 splenic vein thrombosis in one patient given 30 mg/day. The latter was the only grade 3 drug-related adverse event. There were no treatment-related adverse events of grade 3 or higher in patients given 10 or 20 mg/day. In general, the toxic effects of TAC-101 were consistent with those of previous studies.[7,8]

Higginbotham *et al.* reported the results of pharmacokinetic studies of TAC-101 in patients with advanced hepatocellular carcinoma treated in the United States.[8] The mean pharmacokinetic parameters (t_{max}, 4.3 h; C_{max}, 242 ng/mL; AUC_{0-24}, 3067.6 ng h/mL; AUC_{inf}, 4241.1 ng h/mL) obtained for a dose of 20 mg were generally consistent with our data in Japanese patients. The slightly lower C_{max} and AUCs values in the American study might be attributed to general differences in body size between Caucasians and Japanese.

Both maximum (C_{max}) and overall exposures (AUCs) to TAC-101 were generally dose-related within the range of 10 to 30 mg/day. The parent compound TAC-101 was not excreted into urine, suggesting that hepatic metabolism is the major elimination pathway of TAC-101. The primary metabolism of TAC-101 was characterized by hydroxylation of the trimethylsilyl group, producing some primary metabolites, which then underwent glucuronide conjugation. However, the concentrations of the metabolites in plasma were low, suggesting that the biologic activity of TAC-101 is generally attributed to systemic exposure to unchanged TAC-101.

On the basis of the pharmacokinetic and safety profiles of TAC-101 in this study, 20 mg/day, the dose one level below the MTD, was determined to be RD. This dose is the same as the RD in the United States.

As for antitumor effect, no patient had a CR or PR, but nine had NC (69.2%, 9/13 subjects). The median TTF was 60.0 days, the median TTP was 86.0 days, and the MST was 427.0 days. The results for efficacy in this study were also similar to those in the study performed in the United States.[8] Unfortunately, tumor shrinkage was not evident, and the median TTP seemed to be unfavorable on the basis of MST. However, we believe that further evaluations are warranted,